BIOCHEMISTRY
including biophysical chemistry & molecular biology

ARTICLE

pubs.acs.org/biochemistry

Isolation of the Silicatein-α Interactor Silintaphin-2 by a Novel Solid-Phase Pull-Down Assay

Matthias Wiens,*[,†] Heinz-C. Schröder,[†] Xiaohong Wang,[†,‡] Thorben Link,[†] Dominik Steindorf,[†] and Werner E. G. Müller*[,†]

[†]Institute for Physiological Chemistry, University Medical Center of the Johannes Gutenberg-University, Duesbergweg 6, D-55128 Mainz, Germany

[‡]National Research Center for Geoanalysis, 26 Baiwanzhuang Dajie, CHN-100037 Beijing, China

ABSTRACT: The skeleton of siliceous sponges consists of amorphous biogenous silica (biosilica). Biosilica formation is driven enzymatically by means of silicatein(s). During this unique process of enzymatic polycondensation, skeletal elements (spicules) that enfold a central proteinaceous structure (axial filament), mainly comprising silicatein, are formed. However, only the concerted action of silicatein and other proteins can explain the genetically controlled diversity of spicular morphotypes, from simple rods with pointed ends to intricate structures with up to six rays. With the scaffold protein silintaphin-1, a first silicatein interactor that facilitates the formation of the axial filament and, consequently, of the growing spicule was discovered. In this study, a new interactor has been identified by both a conventional yeast two-hybrid library screening and a newly established pull-down assay. For the latter approach, silicatein-α has been bioengineered to carry a Glu tag, which confers binding affinity to hydroxyapatite. After immobilization on a solid-phase matrix (hydroxyapatite), the Glu-tagged silicatein was used as bait for the identification of interactors. Both approaches revealed a 15 kDa polypeptide, and its identity was confirmed by matrix-assisted laser desorption ionization time-of-flight mass spectrometry. Colocalization of silintaphin-2 and silicatein-α within the axial filament and on the spicule surface was shown by immunohistological analyses. Subsequent autoradiography demonstrated the Ca^{2+} binding affinity of this silicatein interactor. These findings indicate that both proteins operate in concert during spiculogenesis. Besides binding of calcium, silintaphin-2 shares several structural features with certain acidic, secreted extracellular matrix proteins that facilitate tissue mineralization in Metazoa. Hence, silintaphin-2 might mediate signal transduction during spiculogenesis or may play a more direct role during biosilica formation, in concert with silicatein.

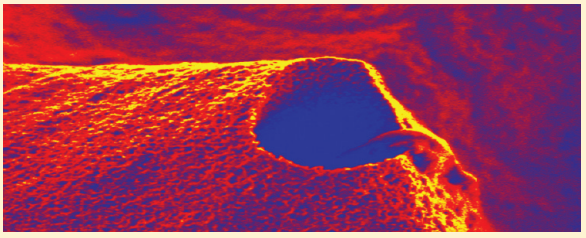

After the extensive study of marine shallow and deep-sea life in the 19th Century, uni- and multicellular organisms with siliceous skeletons were considered the most "beautiful" inhabitants of these particular ecosystems.[1,2] Especially sponges (Porifera) and diatoms were thought to have no "rival in beauty".

The growth of diatom silica frustules[3] and poriferan siliceous spicules[4] is guided by organic matrices. In the inorganic world, polycondensation of silicate to poly(silicate) depends on the saturation state of the monomeric substrates [soluble silica or monomeric orthosilicic acid (H_4SiO_4)] as well as on environmental pH, ionic strength, and temperature.[5−7] In contrast, in biological systems, the physicochemical reactions are accelerated either nonenzymatically (e.g., through silaffins in diatoms[8]) or enzymatically [through silicatein(s) in sponges[9,10]], resulting in the synthesis of biogenous silica (biosilica). The enzyme silicatein, which is related to cathepsin proteases, comprises a catalytic amino acid triad (Ser-His-Asn) in which Ser has replaced the Cys of cathepsins.[11] Consequently, it has been proposed that these amino acids of the catalytic triad facilitate the polycondensation of substrates as siloxane in a manner analogous to that of the catalytically active residues of Ser/Cys-based proteases.[11] This suggestion was supported by the finding that silicatein catalyzes the polycondensation of poly(silicate) from monomeric tetraethoxysilane (TEOS) at neutral pH. Recently, silicatein and silicatein-mediated reactions have gained considerable interest because of the biomedical and biotechnological potential of biosilica (e.g., refs 12−14).

In siliceous sponges, silicatein monomers assemble as a rodlike structure (axial filament) that is located within the siliceous skeletal elements (spicules) in a distinct canal (axial canal) (see ref 15). Whereas the axial filament of marine sponges comprises several silicatein isoforms (silicatein-α, -β, and -γ[16]), the filament of freshwater sponges harbors only isoforms of silicatein-α.[17] The assembly of the different silicatein isoforms to the axial filament during spiculogenesis is stoichiometrically controlled; four silicatein-α molecules assemble symmetrically around a central silicatein-β molecule so that the enzymes' active sites are still accessible.[18] Via fractal-like structures, this initial assembly results in filaments of higher-order patterns that differ between different sponge species.[19] The protein units within the filaments are highly organized and show two different orientations of the lattices formed, spaced by distances of 5.8 nm. The lattice orientations are regular in a two-dimensional

Received: September 3, 2010
Revised: February 10, 2011
Published: February 14, 2011

hexagonal arrangement of protein units, perpendicular to the spicule axis (e.g., in the demosponge *Geodia cydonium*). Alternatively, two different two-dimensional lattices are present, in which the repeating protein units are inclined by a defined angle (e.g., in the hexactinellid *Scolymastra joubini*).[19,20] These findings are supported by the fact that there is a broad range of genetically determined spicular morphotypes.[15]

Initially, it had been proposed that formation of patterned poly(silicate) structures in biological systems is exclusively determined by physicochemical factors, e.g., electromagnetic vibrations.[21] However, with the discovery of silicateins and the subsequent finding that the shape of the axial filament affects spicule morphology, a change in paradigm occurred.[16,22] Additionally, the molecular composition was found to have some significance for spicule morphology.[23] While megascleres of *G. cydonium* comprise all three silicatein isoforms (α, β, and γ), the smaller microscleres contain only one form of silicatein. Finally, different post-translational modifications, e.g., phosphorylation[22] and methylation,[24] might influence not only silicatein activity but also axial filament morphology.

With the scaffold protein silintaphin-1, for the first time a constituent of axial filaments that is not part of the silicatein protein family was discovered.[25] The silicatein interactor silintaphin-1 facilitates and controls not only the assembly of silicatein as filaments but also the assembly of nanoparticles (γ-Fe_2O_3, titania, or silica) as ordered structures.[22] Silintaphin-1 was discovered during a yeast two-hybrid library screening. This system allows a comprehensive and reliable identification of biologically relevant interacting proteins, provided that all available controls have been analyzed.[26] In this study, a new silicatein-interacting protein, silintaphin-2 of the demosponge *Suberites domuncula*, was identified through a yeast two-hybrid library screening. Subsequently, a solid-phase pull-down assay was established, using recombinant silicatein as bait to search for silintaphin-2 in a complementary approach. In this assay, a strong silicatein-interacting prey protein was discovered, which matrix-assisted laser desorption ionization time-of-flight mass spectrometry (MALDI-TOF-MS) revealed to be identical to silintaphin-2, consequently confirming the interaction of silintaphin-2 and silicatein. Then, antibodies against this silicatein interactor were raised and used for immunohistological detection of silintaphin-2, which was discovered to colocalize with silicatein in axial filaments and on spicule surfaces. Finally, recombinant silintaphin-2 was employed to evaluate calcium binding through ^{45}Ca autoradiography.

MATERIALS AND METHODS

Sponge Spicules, Protein Extracts, and Antibodies. Specimens of the marine sponge *S. domuncula* (Porifera, Demospongiae, Hadromerida) were collected in the Northern Adriatic near Rovinj, Croatia, and then kept in aquaria in Mainz, Germany, at a temperature of 17 °C. *S. domuncula* tissue contains only oxeal/styleal spicules. The oxeas (tylostyles) have lengths of 50−350 μm (90−320 μm) with diameters of 4−6 μm (5−8 μm). Spicules were isolated by treatment of the tissue with nitric acid and sulfuric acid.[23] For partial or complete dissolution of biosilica, the spicules were incubated with 50 mL of hydrofluoric acid [1 M HF/4 M NH_4F (pH 5.0)] for 5 min to 3 h, as described previously.[16]

Primmorphs (three-dimensional cell culture) were obtained from single sponge cells and cultivated in natural seawater (Sigma-Aldrich, Taufkirchen, Germany), supplemented with 0.2% RPMI1640 medium at 17 °C.[27] After reaching sizes of 6−8 mm, primmorphs were transferred to a silicate cushion that had been prepared from orthosilicate to accelerate spicule formation.[28] After 3 days, primmorphs were homogenized and proteins extracted in 0.4 M Tris-HCl buffer (pH 8.0) (50 mM NaCl, 0.5 mM EDTA, and 5 mM $MgCl_2$) at 4 °C for 1 h, followed by centrifugation (20000*g*).

The preparation of polyclonal antibodies has been described previously.[22,25] For immunodetection, polyclonal rabbit antibodies directed against silicatein-α (aSilic-α 365; 1:2000 dilution for application in Western blots) or silicatein-β (aSilic-β 363/2; 1:1000) were used. In addition, polyclonal anti-silintaphin-1 antibodies (aSiphn-1-01; 1:3000) that had been raised in female BALB/c mice[25] were employed. Preimmune sera were used as controls. Anti-His antibodies and secondary antibodies were obtained from Invitrogen (Karlsruhe, Germany) and Dianova (Hamburg, Germany).

Electron Microscopy. Scanning electron microscopy (SEM) analysis of spicules was performed with a Zeiss DSM 962 digital scanning microscope (Zeiss, Aalen, Germany) as described previously.[22] For sample analysis by transmission electron microscopy (TEM), the tissue samples were fixed in 0.1 M phosphate buffer (supplemented with glutaraldehyde), as described previously.[22] Where indicated, tissue slices were successively incubated with PoAb-aSilic and a gold-labeled secondary antibody [1.4 nm nanogold anti-rabbit IgG (Nanoprobes, Yaphank, NY)] for 2 h. The samples were inspected with a Tecnai 12 microscope (FEI Electron Optics, Eindhoven, The Netherlands).

Forward Yeast Two-Hybrid Library Screen. The complete cDNA of the *S. domuncula* silicatein-α was cloned as a gene of interest into the pENTR/D-TOPO vector (Invitrogen). The cDNA additionally contained a 5′-CACC fragment to allow directional cloning, followed by a 5′-initiation codon within the context of a Kozak sequence to allow for proper translation initiation, and a 3′-stop codon. Via recombination [catalyzed by LR clonase (Invitrogen)], the *S. domuncula* silicatein-α sequence, then, was transferred into the pDEST32 destination vector, in frame with a sequence encoding the GAL4 DNA binding domain (5′-GAL4 DBD-silicatein-α-3′). The resulting open reading frame (ORF) of the bait construct was confirmed using the Li-Cor 4300 automatic DNA sequenator (Li-Cor Biosciences, Bad Homburg, Germany). Subsequently, MaV203 yeast cells were transformed with a combination of bait (pDEST32/silicatein-α) and prey vector [pDEST22 expression cDNA library containing the GAL4 activation domain (GAL4 AD)], or with ProQuest Two-Hybrid System control bait and prey plasmids, encoding strong, weak, and negative interactors (Invitrogen). Interaction between bait and prey fusion proteins brings together GAL4 DBD and GAL4 AD, resulting in the expression of reporter genes. Positive interactions were detected by selection on media lacking the auxotrophic marker histidine or uracil, by assaying for β-galactosidase activity, and by growth inhibition in the presence of 5-fluoroorotic acid. Following the isolation of prey plasmids from cells displaying the appropriate phenotypes, MaV203 cells were retransformed with silicatein bait and prey plasmids to confirm interaction. Prey plasmid inserts were sequenced and computationally analyzed, using the EMBL-EBI (http://www.ebi.ac.uk/Tools/fasta33/index.html) and NCBI (http://blast.ncbi.nlm.nih.gov/Blast.cgi) servers. Potential subunits,

domains, patterns, and transmembrane regions were predicted, searching Pfam (http://pfam.sanger.ac.uk/), SMART (http://smart.embl-heidelberg.de/), and myHits (http://myhits.isb-sib.ch/cgi-bin/index) databases. The sequence thus identified was termed silintaphin-2, as the second member of a family of silicatein-α interactors.[25]

Preparation of Recombinant Silintaphin-2 and Raising of Anti-Silintaphin-2 Antibodies. The complete open reading frame of silintaphin-2 (nucleotides 87−497), excluding Met_{start} and the stop codon, was amplified with a combination of a forward primer (5′-AAGATTGCTATTTTTGTCCTGGC-3′) and a reverse primer (5′-TCGACCAAGAAATCCTGCTGC-3′). The resulting polymerase chain reaction (PCR) product was T/A cloned into bacterial expression vector pTrcHis2-TOPO (Invitrogen), in frame with an N-terminal Met_{start} and a C-terminal 6xHis tag. Following transformation of BL21 cells (Invitrogen), expression of recombinant protein was induced with 1 mM isopropyl 1-thio-D-galactopyranoside (IPTG) (Sigma-Aldrich, Taufkirchen, Germany) for 6 h. Subsequently, the protein was extracted and purified by nickel-nitrilotriacetic acid (Ni-NTA) affinity chromatography, following the manufacturer's instructions (Qiagen, Hilden, Germany). Protein concentrations were measured with the "2-D Quant Kit" (GE Healthcare, München, Germany). Subsequently, the protein was analyzed by sodium dodecyl sulfate−polyacrylamide gel electrophoresis (SDS−PAGE) and stained with GelCode Blue reagent (Pierce, Rockford, IL). After being blotted on polyvinylidene fluoride membranes (PVDF) (Millipore, Billerica, MA), the recombinant protein was detected with anti-histidine antibodies. Ultimately, purified recombinant silintaphin-2 (15 μg/injection) was used to raise polyclonal antibodies (aSiphn-2-01) in female BALB/c mice as described previously.[29] Preimmune serum was collected as a control.

Preparation of Glu-Tagged Silicatein. Glu-tagged silicatein-α, carrying an additional C-terminal His tag, was prepared as described recently.[30] In short, the cDNA of *S. domuncula* silicatein-α (NCBI accession number AJ272013), encoding the mature enzyme (amino acids 115−330), was amplified with a combination of forward primer 5′-CAT G*CC ATG* GTG GAA GAG GAA GAG GAA GAG GAA GAG CCT GAA GCT GTA GAC TGG-3′ (*Nco*I site italicized, 8xGlu tag underlined) and reverse primer 5′-CCC *AAG CTT* ATT AGG GTG GGA TAA GAT GCA TCG GT-3′ (*Hin*dIII site italicized). PCR was conducted using the method of Natalio et al.[30] The amplicon was inserted into bacterial expression vector pBAD/gIII A (Invitrogen), in frame with vector sequences encoding an N-terminal Met_{start} and a C-terminal 6xHis tag. The construct was used to transform TOP10 *Escherichia coli* cells. Recombinant protein expression was induced with arabinose (0.2%, 24 h). Then, proteins were extracted and purified by Ni-NTA affinity chromatography. The resulting silicatein preparation was found to have a purity of >95%, as checked by SDS−PAGE. Refolding of the protein was induced with a 0.7 M L-arginine buffer (containing 5.0 mM EDTA, 0.1% (v/v) CHAPS {3-[(3-cholamidopropyl)dimethylammonio]-1-propanesulfonate}, 10 mM glutathione, and 1.0 mM glutathione disulfide (pH 7.2)).

^{45}Ca Autoradiography. To assess the Ca^{2+} binding capacity of silintaphin-2, we used the assay described by Maruyama et al.[31] For this purpose, purified recombinant silintaphin-2 was size-separated by SDS−PAGE (0.3−10 μg of protein/lane) and, then, transferred onto a nitrocellulose membrane. After being extensively washed [3 × 20 min; 10 mM imidazole-HCl, 60 mM KCl, and 5 mM $MgCl_2$ (pH 6.8)], the blot was submerged in 10 μM $^{45}CaCl_2$ (1 mCi, 37 MBq; PerkinElmer, Fremont, CA) for 1 h at 20 °C, followed by three washing steps (5 min each) in distilled H_2O. Finally, the membrane was dried at room temperature (2−3 h), before it was exposed to Kodak X-Omat LS film (Sigma-Aldrich). In parallel, immobilized proteins on the blots were stained with Ponceau S.

Pull-Down Assay. For isolation of silicatein interactors, a modified pull-down assay was applied.[32] For this purpose, silicatein was bioengineered to carry both a Glu tag (N-terminal) and a His tag (C-terminal) (see above). Then, the recombinant protein was immobilized on the surface of synthetic hydroxyapatite microparticles (HA; Sigma-Aldrich) with its Glu tag.[30] Thirty milligrams of hydroxyapatite was added to 150 μg of Glu-tagged silicatein in Tris buffered saline (TBS, pH 7.5) and incubated overnight on a shaker (MBI Orbital Shaker) at 4 °C. Then, the particles were pelleted (30 s at 3000*g*) and resuspended in TBS. Subsequently, 500 μL of sponge protein extract (see above; 3 mg/mL protein) was added to the slurry and the mixture incubated for 2 h at 20 °C while being shaken. Afterward, the particles were pelleted again, washed thrice with 20 mM imidazole (pH 7.4), and pelleted one last time. Ultimately, silicatein-bound proteins were eluted with 1 mL of 6 M guanidine (pH 3.3) and analyzed via SDS−PAGE, Western blotting, and MALDI-TOF-MS.

SDS−PAGE, Western Blotting, and MALDI-TOF-MS. For identification of silicatein interactors, proteins that had been bound to silicatein-α during the pull-down assay were eluted and subjected to SDS−PAGE. After size separation and subsequent protein transfer on PVDF membranes, the membranes were incubated with polyclonal antibodies, i.e., anti-silicatein-α (aSilic-α 365; 1:2000 dilution), anti-silicatein-β (aSilic-β 363/2; 1:1000), and anti-silintaphin-1 (aSiphn-1-01; 1:3000). Then, immune complexes were visualized colorimetrically following consecutive incubations with alkaline phosphatase (AP)-conjugated species-specific secondary antibodies and 4-nitro blue tetrazolium chloride (NBT) and 5-bromo-4-chloro-3-indolyl phosphate (BCIP) (Invitrogen). To identify a silicatein interactor that had not been immunodetected by the aforementioned antibodies, a size-separated major band at ca. 15 kDa was excised from the SDS gel, destained, dehydrated in acetonitrile, and dried in a SpeedVac concentrator (Thermo Savant, Brussels, Belgium). Subsequently, the sample was digested with trypsin in ammonium bicarbonate.[33] Then, the peptides were extracted and analyzed by matrix-assisted laser desorption ionization time-of-flight mass spectrometry (MALDI-TOF-MS) as described previously.[33] Spectra were recorded on an Ultraflex MALDI-TOF mass spectrometer and analyzed with FlexControl version 2.2 (Bruker Daltonik, Bremen, Germany).

Immunohistology. Tissue slices of primmorphs were prepared as described previously.[22] Slices of 8 μm were fixed in paraformaldehyde. After the samples had been washed with phosphate-buffered saline (PBS) at room temperature, unspecific binding was blocked with 2% (v/v) goat serum (Invitrogen) and 2% (v/v) gelatin from cold water fish skin (Sigma-Aldrich). Then, the specimens were incubated with primary antibodies, either rabbit anti-silicatein-α (aSilic-α 365) or murine anti-silintaphin-2 polyclonal antibodies, both diluted 1:50 in blocking solution and incubated with shaking at 4 °C overnight. Alternatively, the respective preimmune serum was used as a control. Unbound antibodies were removed when the samples were washed four times with PBS prior to the incubation with

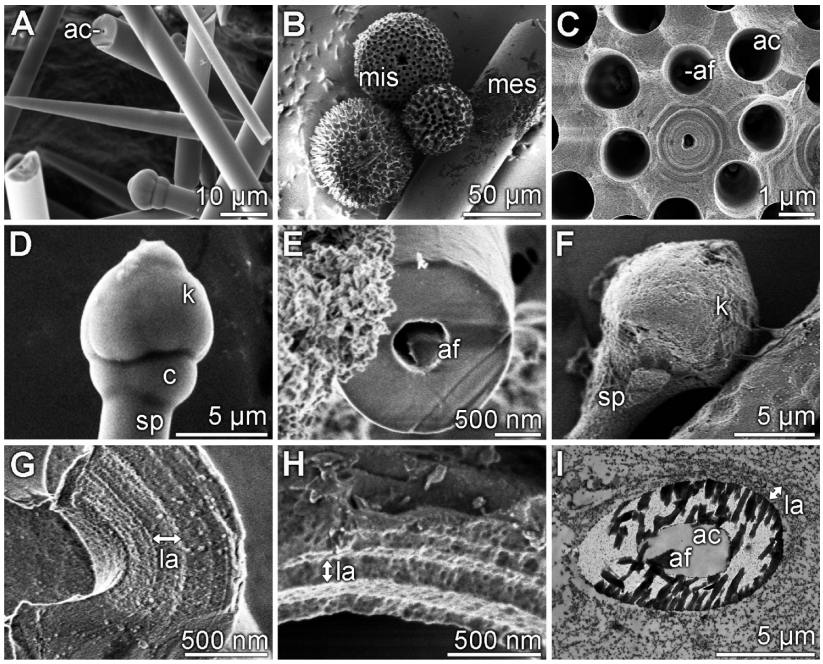

Figure 1. Spicules of the demosponge *S. domuncula* (A and D−I) and *G. cydonium* (B and C). (A) Cluster of tylostyles and oxeas/styles (SEM). One broken spicule shows the axial canal (ac). (B and C) Microscleres (asters) (mis) and one megasclere fragment (mes) (SEM). The asters are composed of many rays that originate from a bulky globular center. In panel C, a cross section of an aster shows its many axial canals (ac); each axial canal is at the center of one ray. In one axial canal, the axial filament (af) can be seen. (D) Rod-shaped monaxonic tylostyle (sp) with a terminal knob (k) that is placed atop a collar (c) (SEM). (E) Cross section of a spicule displaying the axial filament (af) (SEM). (F) Limited dissolution of a spicule (sp), terminated by the knob (k), releases the axial filament (SEM). (G) Limited dissolution of the siliceous mantle of a tylostyle, revealing the concentric stacking of siliceous lamellae (la) (SEM). (H) Cross section of a siliceous mantle, showing the appositional stacking of siliceous lamellae (la) (SEM). (I) Cross section of *S. domuncula* tissue, showing a growing spicule with an axial filament (af) and the surrounding siliceous axial cylinder (ac) (TEM). The combination of anti-silicatein antibodies and gold-labeled secondary antibodies detected silicatein within the axial filament and the surrounding area of the spicule. A concentric accumulation of signals along a newly forming silica layer is marked (la).

species-specific secondary antibodies (1:3000 dilution), fluorescently labeled with Cy3 (Dianova) or Alexa Fluor 488 (Invitrogen). Immunofluorescence was studied with the combination of an Olympus AHBT3 light microscope and an AH3-RFC reflected light fluorescence attachment.

RESULTS AND DISCUSSION

Spicule Morphology. Tissue of the siliceous sponge *S. domuncula* comprises only megascleres (50−350 μm in length), in particular tylostyles (spicules with a globular swelling at one end and a sharp tip at the other) and the less abundant oxeas/styles (pointed at both ends) (Figure 1A). In contrast, the *G. cydonium* skeleton is composed of both microscleres (asters, 30−75 μm) and megascleres (oxeas, ≤ 4 mm) (Figure 1B). While the rod-shaped monaxonic styles have only one central axial canal with a width of 0.8−1.0 μm (Figure 1A,E), the spheroidal asters have a voluminous, globular center from which numerous rays originate (Figure 1B). A cross-sectioned aster shows that each ray contains one axial canal (Figure 1C); in some of the canals, the organic axial filament can be identified. The *S. domuncula* tylostyles are characterized by a surprisingly regular shape, with diameters of 6.5−7.3 μm (Figure 1D). Most of the tylostyles have subterminal collars (6.9−7.2 μm). A cross section of a tylostyle shows the triangular axial filament (Figure 1E). After limited dissolution with HF, it is seen that the axial filament is terminated by a pinheadlike structure (Figure 1F). Following a short exposure (10 min) of cross-sectioned spicules to HF, a layered pattern of the silica mantle can be observed; the layer thickness is ∼50 nm (Figure 1G,H). Immunodetection with nanogold-labeled antibodies highlights the presence of silicatein not only within the axial filament but also within the extracellular matrix close to spicules (Figure 1I).

Identification of the Silicatein-α Interactor Silintaphin-2 by Yeast Two-Hybrid Library Screening. To identify silicatein binding partners, the cDNA encoding mature silicatein-α was ligated in bait vector pDEST32, in frame with the GAL4 DNA binding domain. Then, MaV203 yeast cells were cotransformed with both the resulting construct and a prey vector that was part of a pDEST22 expression cDNA library, containing the GAL4 activation domain. Only in those cells, where prey and bait protein interacted, was expression of the reporter genes induced. Hence, on selective plates, colonies that were β-galactosidase positive and unable to grow in the presence of 5-fluoroorotic acid were formed. Comparisons with the growth profile and promptness of the β-galactosidase-catalyzed reaction of yeast controls (transformed with control bait and prey plasmids) revealed a strong silicatein-α interactor. Subsequently, prey-bearing plasmids were isolated from five yeast colonies and their inserts sequenced. The SDSIPHN-2-termed cDNA insert comprised 665 nucleotides [excluding the poly(A) tail]. This size was confirmed by Northern blot analysis [0.7 kb (data not shown)]. One ORF could be deduced from nucleotides 84−86 (Met_{start}) to nucleotides 498−500 ($stop_{TGA}$), putatively encoding a protein of 138 amino acids (SIPHN-2_SUBDO) with an expected size of 15506.35 Da (isoelectric point of 4.50) (Figure 2). A

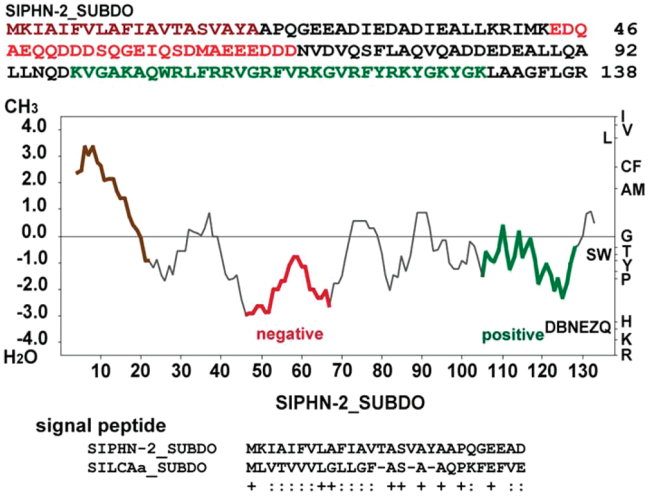

Figure 2. *S. domuncula* silicatein interactor silintaphin-2. (A) Amino acid sequence (SIPHN-2_SUBDO) deduced from the SDSIPHN-2 ORF. SIPHN-2_SUBDO comprises three regions, the N-terminal signal peptide (brown) and two highly charged clusters [negatively (red) and positively (green) charged]. The Kyte−Doolittle hydrophobicity/hydrophilicity plot shows the location of the charged segments within the highly hydrophilic protein. Below the plot, an alignment of the N-termini of silintaphin-2 (SIPHN-2_SUBDO) and *S. domuncula* silicatein-α (SILCAa_SUBDO) is shown, indicating significant sequence similarity. Residues with identical physicochemical properties (+) or similar properties (:) are marked.

database search (e.g., NCBI-Blast) revealed no significant homology [expect value (*E* value[34]) of $<10^{-3}$] between SDSIPHN-2 and deposited sequences. This result indicates that silintaphin-2 should be allocated to the set of sponge/*S. domuncula*-specific transcripts, amounting to 34% of the transcriptome (deduced for >10000 sequenced *S. domuncula* ESTs[35]). Noticeable is the high percentage of charged amino acid residues, with >20% negatively (Asp and Glu) and 13% positively (Arg and Lys) charged residues, as well as the presence of numerous Gln residues. Applying the algorithm of Kyte and Doolittle[36] (http://fasta.bioch.virginia.edu/fasta_www2/fasta_www.cgi?rm=misc1) for the prediction of hydrophobic/hydrophilic segments, we find two pronounced hydrophilic regions within the silintaphin-2 sequence. The first one (amino acids 44−69) comprises clusters of negatively charged residues, whereas the second one (amino acids 98−130) features positively charged clusters (Figure 2). No mixed charge clusters are present. In addition, the N-terminus of silintaphin-2 harbors a putative signal sequence (amino acids 1−20) with a cleavage site between amino acids 20 and 21 (http://wolfpsort.org/). It is important to note that the amino acid sequence of the silintaphin-2 signal is significantly homologous to that of the *S. domuncula* silicatein-α signal (GenBank accession number CAC03737.1). Alignment of the two N-terminal sequence stretches revealed nine amino acid residues with identical and 12 residues with similar physicochemical properties (Figure 2). This finding indicates colocalization of both proteins and/or a functional relationship.[37] Furthermore, the putative silintaphin-2 signal is homologous to sequences of a number of metazoan proteins that are secreted and/or transmembrane, e.g., *Simulium vittatum* secreted protein (GenBank entry ACH56863; 61% identical and 61% similar residues), *Glossina morsitans* secreted salivary phospholipase A2 (GenBank entry ADD19849; 47% identical and 52% similar), and *Lytechinus variegates* biomineralization protein P16 (GenBank entry AAY59533; 52% identical and 76% similar). Interestingly, the latter protein represents a transmembrane regulator of skeletogenesis in sea urchins, similar in size to silintaphin-2 and rich with aspartic acid residues. P16 regulates the growth of calcite spicules in sea urchins at a late stage of skeletogenesis, i.e., spicule elongation. The underlying mechanism is still unknown, but similar to osteonectin and other mineralizing proteins, p16 might be involved in both signal transduction and regulation of calcium transport.[38] Similarly, silintaphin-2 might be required during Ca^{2+}-mediated extracellular signaling pathways and mineralization mechanisms. To shed light on the putative role of silintaphin-2 during poriferan spiculogenesis, it is important to assess whether it interacts with calcium and to analyze the in situ localization of this poriferan protein (see below).

Identification of Silintaphin-2 by Pull-Down Assay and Coupled MALDI-TOF-MS. From a recent study, we know that an N-terminal sequence of eight Glu residues confers high binding affinity to solid-phase hydroxyapatite (HA).[30] Hence, Glu-tagged and HA-immobilized proteins might be employed to isolate thus-far unknown interactors through a solid-phase pull-down assay; a schematic outline is given in Figure 3. In our study, Glu-tagged and HA-immobilized silicatein-α was incubated with primmorph protein extracts to identify new silicatein-α interactors. Primmorphs represent a special type of three-dimensional cell culture and have been shown to intensely synthesize spicules and proteins involved in spiculogenesis.[28,39] Following extensive washing to remove unbound proteins, putative silicatein interactors were eluted with guanidine. Eluted proteins, then, were size-separated via SDS−PAGE. After being blotted on PVDF membranes, known interactors of silicatein-α were detected immunologically with their respective polyclonal antisera. Accordingly, silintaphin-1 was detected at the expected size of 43 kDa (Figure 4A, lane a); the corresponding preimmune serum did not react with any protein (lane b). Similarly, a 35 kDa protein was identified with antisilicatein-α antibodies, corresponding to the unprocessed form of the silicatein-α (Figure 4A, lane c). Unprocessed silicatein-α is prevalent in the extracellular matrix, the mesohyl. Only after binding to the spicule surface and the growing axial filament is the proenzyme converted to the mature 24 kDa silicatein-α. The axial filament comprises only this processed, mature form of silicatein.[22] Again, the preimmune serum did not elicit unspecific signals (lane d). Subsequently, silicatein-β was identified within the batch of eluted proteins, with a size of 40 kDa (Figure 4A, lane e), indicative of the unprocessed proenzyme (mature silicatein-β, 24 kDa). Preimmune serum was not reactive (lane f). Finally, through the application of murine aSiphn-2-01 antibodies (raised against the yeast two-hybrid prey), silintaphin-2 was detected on the Western blots [15 kDa (Figure 4A, lane g)], whereas preimmune serum did not cross react (lane h). The corresponding SDS gel displayed major bands that matched the sizes of the immunodetected silicateins and silintaphins (Figure 4B). However, additional bands indicated the presence of further, so far unidentified silicatein indicators that might be unrelated to silicatein and silintaphin.

To confirm the identity of silintaphin-2, in a complementary approach, we excised the 15 kDa protein band from the gel, digested it, and sequenced it de novo using BioTools version 2.2 with RapidDeNovo extension. Two fragments were obtained with probability scores of 91−100%, VGAKAQWR and VGRFVR,

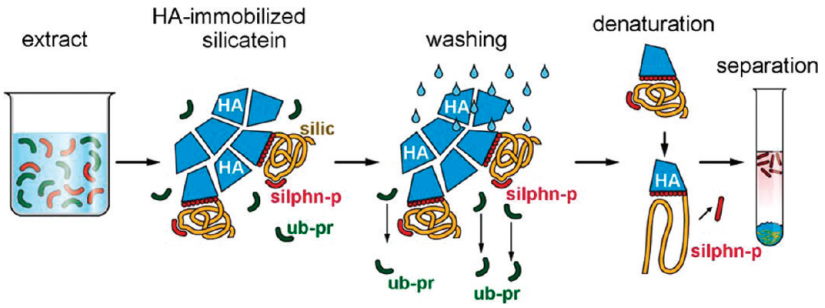

Figure 3. Scheme of a novel solid-phase pull-down assay to identify interactors (prey) of hydroxyapatite-immobilized Glu-tagged proteins (bait). For isolation of putative silicatein interactors (silphn-p), sponge protein extracts were incubated with refolded, hydroxyapatite (HA)-immobilized Glu-tagged silicatein (silic). Following incubation, unbound proteins (ub-pr) were removed via several washing steps. Finally, the slurry was suspended in guanidine buffer, for denaturation and release of silicatein, and its interactors were, subsequently, separated from the the solid phase by centrifugation.

corresponding to amino acids 99−106 and 111−116, respectively, of the protein sequence that had been identified through yeast two-hybrid library screening.

These results confirmed the functional principle of this novel pull-down assay, i.e., the detection of protein interactors through Glu-tagged and HA-immobilized bait. In addition, they corroborated previous results, showing tetramerization of silicatein-α subunits and subsequent binding to silicatein-β and silintaphin-1 during axial filament formation.[18,25] Lastly, they indicated that extracellular silicatein monomers remain unprocessed and are converted to only the mature, enzymatically active form immediately before their assembly as axial filaments. Thus, it was not surprising that mature silicatein was not detected during this pull-down assay because only extracts of soluble proteins were prepared and mature silicatein likely remained attached to biosilica and axial filaments.

Expression of *S. domuncula* Silintaphin-2. The complete *S. domuncula* silintaphin-2 sequence was expressed in *E. coli*, fused to a His tag. Following isolation through Ni-NTA affinity chromatography, the recombinant protein was analyzed by SDS−PAGE to confirm its purity (Figure 5A, lane a). Subsequently, recombinant silintaphin-2 was detected by anti-His antibodies on Western blots (Figure 5B, lane a) at the expected size of 20 kDa (~5 kDa larger in size than the wild-type protein because of the presence of the His tag and other vector-specific amino acid residues). The purified protein, then, was used to raise murine polyclonal antibodies (aSiphn-2-01). Application of these antibodies once more allowed detection of the recombinant protein on Western blots with a unique band at the expected size (Figure 5B, lane b). As a control, murine preimmune serum was used, which failed to detect the protein (Figure 5B, lane c).

Ca^{2+} Binding of Silintaphin-2. The degree of sequence homology between secretory calcium-binding proteins is usually low, and the binding of Ca^{2+} ions may have a diversity of functions. Thus, calcium binding might induce conformational changes, contribute to enzyme catalysis, or facilitate binding of diverse ligands.[40] Nevertheless, secretory calcium-binding proteins often share several structural characteristics. (i) They carry many charged amino acids (in particular negatively charged amino acids that associate with calcium ions). (ii) They are initially synthesized as precursor proteins comprising an N-terminal signal peptide. (iii) They have an α-helical conformation with an N-terminal β-sheet. (iv) They have few to no cysteine residues but often include many Gln, Pro, and Ser residues (e.g., refs 41−44). Protein regions with this amino acid content facilitate protein binding or binding to ions and crystals.[45]

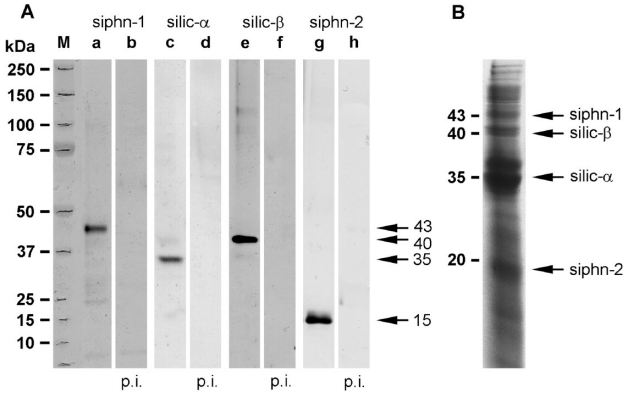

Figure 4. Immunodetection of silicatein-α interactors by a solid-phase pull-down assay coupled to SDS−PAGE and Western blotting. Following incubation of HA-immobilized Glu-tagged silicatein with protein extracts of *S. domuncula* primmorphs, interactors were eluted as described, size-separated by SDS−PAGE, and blotted on membranes. Then, the blots were probed for known interactors with polyclonal antisera. As controls, the respective preimmune sera were employed. (A) Immunoblot: lane a, aSiphn-1-01, detecting silintaphin-1 at 43 kDa; lane b, corresponding preimmune serum (p.i.); lane c, aSilic-α 365, detecting silicatein-α at 35 kDa; lane d, preimmune serum (p.i.); lane e, aSilic-β 363/2, detecting silicatein-β at 40 kDa; lane f, preimmune serum (p.i.); lane g, aSiphn-2-01, detecting silintaphin-2 at 15 kDa; lane h, preimmune serum. (B) SDS−PAGE. Among the different proteins eluted from HA-immobilized Glu-tagged silicatein, the bands corresponding to silicateins and silintaphins are predominant (marked). However, additional major bands indicate the presence of further, so far unidentified silicatein indicators.

All of the features mentioned above apply to silintaphin-2 (Figure 6A). Thus, analysis and prediction of the secondary structure revealed that the protein primarily comprises a helical structure that is interrupted by several turns. These regions contain numerous charged amino acids; two clusters (negatively and positively charged) can be distinguished. In addition, an N-terminal signal sequence has been predicted. Moreover, ~12% of the sequence consists of Gln, Pro, and Ser residues, but no Cys residue is present. Finally, silintaphin-2 displays an N-terminal β-sheet that, for example, in osteocalcin exhibits chemoattractant activity toward osteoclast precursors.[41]

To assess putative silintaphin-2 calcium binding affinity, different concentrations of the recombinant protein were subjected to SDS−PAGE. Then, the proteins were blot-transferred and the membranes incubated with $^{45}CaCl_2$ (Figure 6B1).

Following exposure to the membranes, autoradiographs depicted strong signals in samples that contained 10 and 3 μg of protein (Figure 6B1, lanes a and b, respectively). With 0.3 μg of silintaphin-2, no distinct signal could be resolved (lane c). For comparison, 3 μg of recombinant silicatein had been size-separated on the same gel and blotted subsequently but elicited no signal (lane d, 26 kDa). After autoradiography, the same membrane was incubated with Ponceau S to stain all proteins (Figure 6B2). Clear bands were detected in samples in which 10 and 3 μg of silintaphin-2 per lane had been applied (lanes a and b) as well as 3 μg of silicatein per lane (lane d). However, 0.3 μg of silintaphin-2 (lane c) was below the detection limit.

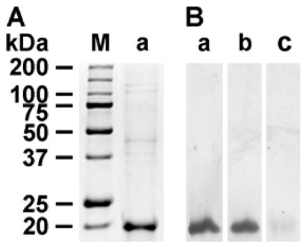

Figure 5. Recombinant silintaphin-2. (A) The Ni-NTA affinity-purified polypeptide was separated by SDS−PAGE and stained with Coomassie Brilliant Blue (lane a) (M, size marker). (B) After size separation, the protein was transferred onto PVDF membranes and probed with anti-His (lane a) or anti-silintaphin-2 antibodies (lane b). Immunocomplexes were visualized with labeled secondary antibodies. As a control, the blot was incubated with preimmune serum (lane c) that elicited no cross reaction.

In Situ Localization of Silintaphin-2. To assess in situ localization of silintaphin-2 and its putative colocalization with silicatein-α, primmorph sections were treated either with murine anti-silintaphin-2 polyclonal antibodies or with rabbit anti-silicatein-α polyclonal antibodies. Following detection with species-specific secondary antibodies [Alexa Fluor 488-conjugated anti-mouse (Figure 7A,D,G) or Cy3-conjugated anti-rabbit (Figure 7B,E,H)], subsequent fluorescence micrographs depicted a distinct colocalization of silintaphin-2 and silicatein-α (Figure 7C,F,I). In particular, spicule cross sections revealed colocalization of both proteins not only within axial filaments but also on spicule surfaces. This finding was not surprising, because previous studies documented growth of spicules in two directions, axial and transversal.[22] While axial growth is controlled by elongation of the axial filament, the lateral thickening of the spicules proceeds by appositional layering of silicatein-containing units.[46]

With silintaphin-2, a second interactor for silicatein(s) has been identified. Silintaphin-1 has been proposed to interact with silicatein via its pleckstrin homology (PH) domain.[25] PH

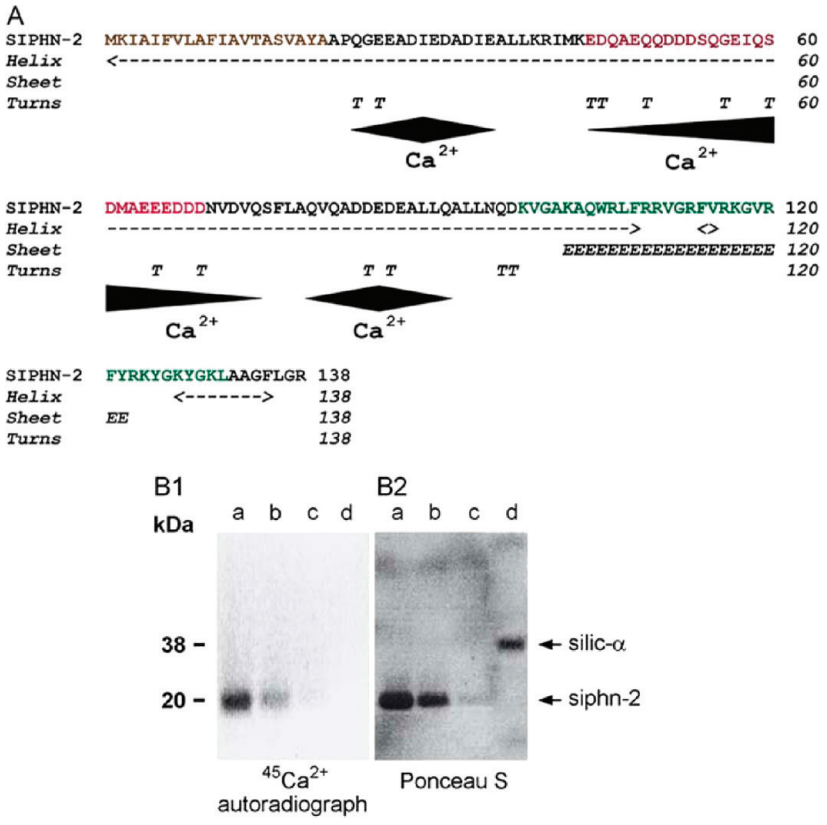

Figure 6. Ca^{2+} binding of silintaphin-2. (A) Predicted secondary structure. The N-terminal signal peptide (brown), the negatively charged amino acid cluster (red), and the positively charged amino acid cluster (green) are marked. Silintaphin-2 (SIPHN-2) has an overall helical secondary structure (↔); only at the N-terminus are β-sheets (E) predominant. Furthermore, the helical region is interrupted by segments that are rich in turns (T). Putative Ca^{2+}-binding regions are marked (diamonds, Ca^{2+}). (B) Ca^{2+} binding measured by incubation of recombinant, size-separated (SDS−PAGE), and blot-immobilized silintaphin-2 with $^{45}CaCl_2$ and subsequent autoradiography. Recombinant silintaphin-2 (10 μg, lane a; 3 μg, lane b; 0.3 μg, lane c) and recombinant silicatein-α (3 μg, lane d) were employed. (B1) Autoradiography. (B2) Protein staining with Ponceau S on the same membrane to verify the applied protein concentrations.

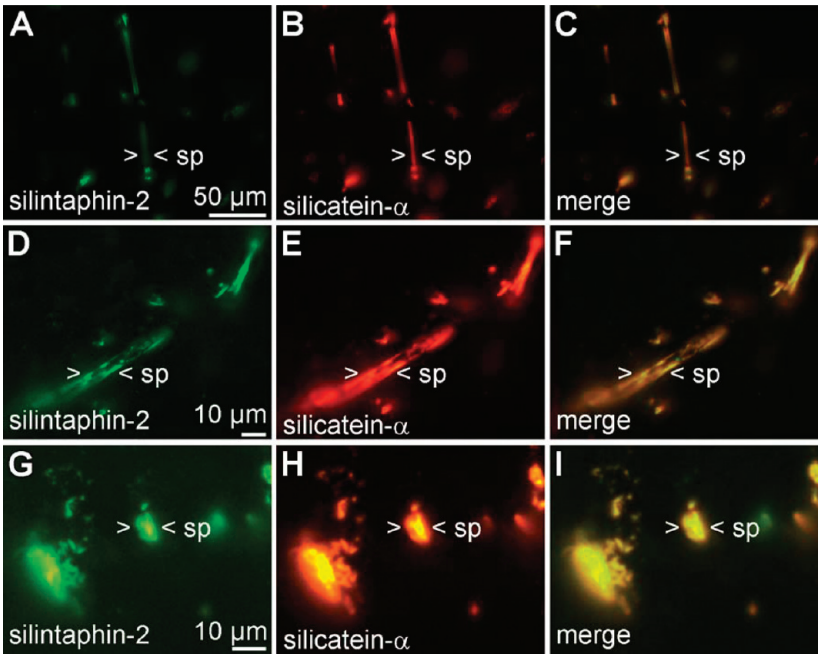

Figure 7. Colocalization of silintaphin-2 and silicatein-α. *S. domuncula* primmorph sections were co-incubated with anti-silintaphin-2 and anti-silicatein-α polyclonal antisera. Immunocomplexes were visualized through treatment with Cy3-conjugated (red) or Alexa Fluor 488-conjugated (green) species-specific secondary antibodies. The merged images reveal a significant colocalization of both proteins (yellow). (A−C) Tissue section overview comprising intensively stained longitudinally sectioned and cross-sectioned spicules (sp). (D−F) Magnification of a longitudinally sectioned spicule. Both silintaphin-2 (green) and silicatein-a (red) manifest in the axial filament and in a proteinaceous layer surrounding the spicule. (G−I) Magnification of a cross-sectioned spicule, depicting colocalization of both proteins.

domains are found in a variety of eukaryotic proteins of multiple families. They mediate interaction with membrane-associated molecules (e.g., phosphoinositides) by forming structures that serve as a scaffold for presenting different types of binding sites.[47,48] Other PH domains recognize protein ligands through their phosphotyrosine site(s). In particular, a positively charged region within the PH domain was reported to facilitate protein−protein interactions.[49] Because silicatein-α has a number of putative phosphorylation sites and clusters of negatively charged amino acid residues, this mechanism of interaction might apply for the interaction of silicatein with silintaphin-1 during the formation of axial filaments. Hence, pentameric units of four silicatein-α molecules and one silicatein-β molecule might be interconnected and/or assembled in the presence of silintaphin-1 (manuscript to be published). In this context, confocal laser scanning has already shown a modular organization of the axial filament in which each module consists of a silintaphin-1 core that is surrounded by silicatein.[25]

Putative Role of Silintaphin-2 during Biosilica Synthesis and Spiculogenesis. The function of silintaphin-2 remains enigmatic so far. However, because silintaphin-2 binds calcium, colocalizes with extracellular silicatein in siliceous spicules, and is significantly similar in structurs to secretory calcium-binding mineralizing proteins, a bi- or even multifunctional role similar to the role of those proteins that are present and operate within the organic matrices of metazoan mineralized tissues can be proposed. One scenario predicts the direct involvement of silintaphin-2 in silica synthesis. In this case, calcium binding of secreted silintaphin-2 induces conformational changes that facilitate binding of silicate, i.e., of the silicatein substrate. Subsequent interaction of silicatein with silicate-loaded silintaphin-2, during elongation of the axial filament or appositional layering of spicules, assists the transport of silicate to the silicatein active site. Hence, silintaphin-2 increases the silicate concentration in the vicinity of silicatein. This protein-mediated, locally restricted enrichment of silicate might be required because the silicate concentration in seawater usually is low ($\leq$10 μM[50]) and spiculogenesis occurs preferentially at silicate concentrations between 5 and 100 μM.[51] The silicon content [as silicon dioxide (from a sponge species not containing spicules, *Spongia officinalis*)[52]] in sponge tissue is relatively high with 1.3% in dry ash, if compared with the nitrogen content in sponges, which amounts to 18.4%.[53]

In a different scenario, silintaphin-2 is only indirectly involved in mineralization. In this case, the protein assumes a hormone-like and/or cytokine-like role, influencing the activity of poriferan mineralizing cells (sclerocytes). Before or after binding to silicatein, calcium once more induces conformational changes, exposing the N-terminal sclerocyte-attracting domain. Consequently, sclerocytes are increasingly attracted to the growing spicules where they participate in the elongation of the axial filament and the growth of spicules.

To distinguish among these hypotheses concerning silintaphin-2 function, future efforts will aim to evaluate whether (i) the poriferan protein interacts directly with silicate, (ii) post-translational modifications of silintaphin-2 contribute to the binding of silicate, (iii) calcium induces conformational changes in silintaphin-2, and (iv) silintaphin-2 has a cell-surface receptor.

CONCLUSION

Poriferan biosilicification represents a unique system for studying the formation of complex biogenous silica structures, from the molecular and genetic basis to the macromolecular

biomaterial. Silicateins enzymatically mediate the conversion of monomeric silicate to poly(silicate) and, hence, are a fundamental prerequisite for the synthesis of biosilica. However, other proteins are crucially involved in the formation and morphogenesis of the elaborately shaped micro- and macroscale skeletal elements. Using hydroxyapatite-immobilized and bioengineered silicatein-α, a novel silicatein interactor and building block of spiculogenesis has been discovered, silintaphin-2. This calcium-binding protein is part of the organic matrix of mineralized sponge tissue and might stimulate the activity of mineralizing cells like other secreted acidic metazoan proteins with hormone and/or cytokine signaling functions. Alternatively, silintaphin-2 might contribute to spiculogenesis in a more direct way by facilitating the polymerizing activity of silicatein. Numerous approaches attempt to mimic and derivatize poriferan biosilicification for the development of novel biomedical and biotechnological applications. Hence, silintaphin-2 represents a new tool for harnessing biosilicification and, consequently, creating tailored siliceous composites in vitro, under nearly physiological conditions.

Accession Codes

The silintaphin-2 sequence of *Suberites domuncula* (SIPHN-2_SUBDO; accession number FR681734) has been deposited (EMBL/GenBank).

AUTHOR INFORMATION

Corresponding Author

*Institute for Physiological Chemistry, University Medical Center of the Johannes Gutenberg-University, Duesbergweg 6, D-55128 Mainz, Germany. Telephone: +49 6131-39-25910. Fax: +49 6131-39-25243. E-mail: wiens@uni-mainz.de (M.W.) or wmueller@uni-mainz.de (W.E.G.M.).

Funding Sources

W.E.G.M. is a holder of an ERC Advanced Investigator Grant (268476 BIOSILICA). This work was supported by grants from the European Commission, the Bundesministerium für Bildung und Forschung (project "Center of Excellence *BIOTEC*marin"), the Deutsche Forschungsgemeinschaft (Schr 277/10-1), the International Human Frontier Science Program, the European Commission, the Johannes Gutenberg-University Research Center for Complex Matter (COMATT), and the International S&T Cooperation Program of China (Grant 2008DFA00980).

REFERENCES

(1) Kützing, F. T. (1844) *Die kieselschaligen Bacillarien oder Diatomeen*, Nordhausen.

(2) Campbell, G. (1876) *Log letters from "The Challenger"*, Macmillan, London.

(3) Kröger, N., Deutzmann, R., and Sumper, M. (2001) Silica precipitating peptides from diatoms: The chemical structure of silaffin-1A from *Cylindrotheca fusiformis*. *J. Biol. Chem. 276*, 26066–26070.

(4) Minchin, E. A. (1909) Sponge-spicules: A summary of present knowledge. *Ergeb. Fortschr. Zool. 2*, 171–274.

(5) Iler, R. K. (1979) *The colloid chemistry of silica and silicates*, Cornell University Press, Ithaca, NY.

(6) Perry, C. C. (2003) Silicification: The processes by which organisms capture and mineralize silica. *Rev. Mineral. Geochem. 54*, 291–327.

(7) Icopini, G. A., Brantley, S. L., and Heaney, P. J. (2005) Kinetics of silica oligomerization and nanocolloid formation as a function of pH and ionic strength at 25 °C. *Geochim. Cosmochim. Acta 69*, 293–303.

(8) Poulsen, N., and Kröger, N. (2004) Silica morphogenesis by alternative processing of silaffins in the diatom *Thalassiosira pseudonana*. *J. Biol. Chem. 279*, 42993–42999.

(9) Cha, J. N., Shimizu, K., Zhou, Y., Christiansen, S. C., Chmelka, B. F., Stucky, G. D., and Morse, D. E. (1999) Silicatein filaments and subunits from a marine sponge direct the polymerization of silica and silicones in vitro. *Proc. Natl. Acad. Sci. U.S.A. 96*, 361–365.

(10) Krasko, A., Batel, R., Schröder, H. C., Müller, I. M., and Müller, W. E. G. (2000) Expression of silicatein and collagen genes in the marine sponge *Suberites domuncula* is controlled by silicate and myotrophin. *Eur. J. Biochem. 267*, 4878–4887.

(11) Morse, D. E. (1999) Silicon biotechnology: Harnessing biological silica production to construct new materials. *Trends Biotechnol. 17*, 230–232.

(12) Schröder, H. C., Boreiko, O., Krasko, A., Reiber, A., Schwertner, H., and Müller, W. E. G. (2005) Mineralization of SaOS-2 cells on enzymatically (silicatein) modified bioactive osteoblast-stimulating surfaces. *J. Biomed. Mater. Res., Part B 75*, 387–392.

(13) Müller, W. E. G., Wang, X., Cui, F. Z., Jochum, K. P., Tremel, W., Bill, J., Schröder, H. C., Natalio, F., Schlossmacher, U., and Wiens, M. (2009) Sponge spicules as blueprints for the biofabrication of inorganic-organic composites and biomaterials. *Appl. Microbiol. Biotechnol. 83*, 397–413.

(14) Wiens, M., Wang, X., Schröder, H. C., Kolb, U., Schlossmacher, U., Ushijima, H., and Müller, W. E. G. (2010) The role of biosilica in the osteoprotegerin/RANKL ratio in human osteoblast-like cells. *Biomaterials 31*, 7716–7725.

(15) Uriz, M. J. (2006) Mineral spiculogenesis in sponges. *Can. J. Zool. 84*, 322–356.

(16) Shimizu, K., Cha, J., Stucky, G. D., and Morse, D. E. (1998) Silicatein α: Cathepsin L-like protein in sponge biosilica. *Proc. Natl. Acad. Sci. U.S.A. 95*, 6234–6238.

(17) Wiens, M., Wrede, P., Grebenjuk, V. A., Kaluzhnaya, O. V., Belikov, S. I., Schröder, H. C., and Müller, W. E. G. (2009) Towards a molecular systematics of the Lake Baikal/Lake Tuva Sponges. In *Biosilica in Evolution, Morphogenesis, and Nanobiotechnology* (Müller, W. E. G., and Grachev, M. A., Eds.) Progress in Molecular and Subcellular Biology Series (Marine Molecular Biotechnology), Vol. 47, pp 111−144, Springer-Verlag, Berlin.

(18) Müller, W. E. G., Boreiko, A., Schlossmacher, U., Wang, X. H., Tahir, M. N., Tremel, W., Brandt, D., Kaandorp, J. A., and Schröder, H. C. (2007) Fractal-related assembly of the axial filament in the demosponge *Suberites domuncula*: Relevance to biomineralization and the formation of biogenic silica. *Biomaterials 28*, 4501–4511.

(19) Croce, G., Frache, A., Milanesio, M., Marchese, L., Causà, M., Viterbo, D., Barbaglia, A., Bolis, V., Bavestrello, G., Cerrano, C., Benatti, U., Pozzolini, M., Giovine, M., and Amenitsch, H. (2004) Structural characterization of siliceous spicules from marine sponges. *Biophys. J. 86*, 526–534.

(20) Croce, G., Frache, A., Milanesio, M., Viterbo, D., Bavestrello, G., Benatti, U., Giovine, M., and Amenitsch, H. (2003) Fiber diffraction study of spicules from marine sponges. *Microsc. Res. Tech. 62*, 378–381.

(21) Thompson, D'Ary W. (1942) *On Growth and Form*, University Press. Cambridge, U.K.

(22) Müller, W. E. G., Rothenberger, M., Boreiko, A., Tremel, W., Reiber, A., and Schröder, H. C. (2005) Formation of siliceous spicules in the marine demosponge *Suberites domuncula*. *Cell Tissue Res. 321*, 285–297.

(23) Müller, W. E. G., Schlossmacher, U., Eckert, C., Krasko, A., Boreiko, A., Ushijima, H., Wolf, S. E., Tremel, W., and Schröder, H. C. (2007) Analysis of the axial filament in spicules of the demosponge *Geodia cydonium*: Different silicatein composition in microscleres [asters] and megascleres [oxeas and triaenes]. *Eur. J. Cell Biol. 86*, 473–487.

(24) Armirotti, A., Damonte, G., Pozzolini, M., Mussino, F., Cerrano, C., Salis, A., Benatti, U., and Giovine, M. (2009) Primary structure and post-translational modifications of silicatein β from the marine sponge *Petrosia ficiformis* (Poiret, 1789). *J. Proteome Res. 8*, 3995–4004.

(25) Wiens, M., Bausen, M., Natalio, F., Link, T., Schlossmacher, U., and Müller, W. E. G. (2009) The role of the silicatein-α interactor silintaphin-1 in biomimetic biomineralization. *Biomaterials 30*, 1648–1656.

(26) Rajagopala, S. V., Hughes, K. T., and Uetz, P. (2009) Benchmarking yeast two-hybrid systems using the interactions of bacterial motility proteins. *Proteomics 9*, 5296–5302.

(27) Müller, W. E. G., Wiens, M., Batel, R., Steffen, R., Borojevic, R., and Custodio, R. M. (1999) Establishment of a primary cell culture from a sponge: Primmorphs from *Suberites domuncula*. *Mar. Ecol. Prog. Ser. 178*, 205–219.

(28) Müller, W. E. G., Kasueske, M., Wang, X. H., Schröder, H. C., Wang, Y., Pisignano, D., and Wiens, M. (2009) Luciferase a light source for the silica-based optical waveguides (spicules) in the demosponge *Suberites domuncula*. *Cell. Mol. Life Sci. 66*, 537–552.

(29) Harlow, E., and Lane, A. (1988) *Antibodies: A Laboratory Manual*, Cold Spring Harbor Laboratory Press, Plainview, NY.

(30) Natalio, F., Link, T., Müller, W. E. G., Schröder, H. C., Cui, F. Z., Wang, X., and Wiens, M. (2010) Bioengineering of the silica-polymerizing enzyme silicatein-α for a targeted application to hydroxyapatite. *Acta Biomater. 6*, 3720–3728.

(31) Maruyama, K., Mikawa, T., and Ebashi, S. (1984) Detection of calcium binding proteins by ^{45}Ca autoradiography on nitrocellulose membrane after sodium dodecyl sulfate gel electrophoresis. *J. Biochem. 95*, 511–519.

(32) Ronemus, M. (2004) Detection of protein-protein interactions using the GST fusion protein pull-down technique. *Nat. Methods 1*, 275–276.

(33) He, J. T., Liu, Y. S., He, S. Z., Wang, Q. S., Put, H., and Ji, J. G. (2007) Proteomic analysis of a membrane skeleton fraction from human liver. *J. Proteome Res. 6*, 3509–3518.

(34) Coligan, J. E., Dunn, B. M., Ploegh, H. L., Speicher, D. W., and Wingfield, P. T. (2000) *Current Protocols in Protein Science*, pp 2.0.1−2.8.17, John Wiley & Sons, Chichester, U.K.

(35) Harcet, M., Roller, M., Cetkovic, H., Perina, D., Wiens, M., Müller, W. E. G., and Vlahovicek, K. (2010) Demosponge EST sequencing reveals a complex genetic toolkit of the simplest metazoans. *Mol. Biol. Evol. 27*, 2747–2756.

(36) Kyte, J., and Doolittle, R. F. (1982) A simple method for displaying the hydrophobic character of a protein. *J. Mol. Biol. 157*, 105–132.

(37) Patthy, L. (1999) *Protein Evolution*, Blackwell Science, Oxford, U.K.

(38) Cheers, M. S., and Ettensohn, C. A. (2005) P16 is an essential regulator of skeletogenesis in the sea urchin embryo. *Dev. Biol. 283*, 384–396.

(39) Müller, W. E. G., Boreiko, A., Brandt, D., Osinga, R., Ushijima, H., Hamer, B., Krasko, A., Xupeng, C., Müller, I. M., and Schröder, H. C. (2005) Selenium affects biosilica formation in the demosponge *Suberites domuncula*: Effect on gene expression and spicule formation. *FEBS J. 272*, 3838–3852.

(40) Maurer, P., Hohenester, E., and Engel, J. (1996) Extracellular calcium-binding proteins. *Curr. Opin. Cell Biol. 8*, 609–617.

(41) Hauschka, P. V. (1986) Osteocalcin: The vitamin K-dependent Ca^{2+}-binding protein of bone matrix. *Haemostasis 16*, 258–272.

(42) Huq, N. L., Cross, K. J., Ung, M., and Reynolds, E. C. (2005) A review of protein structure and gene organisation for proteins associated with mineralised tissue and calcium phosphate stabilisation encoded on human chromosome 4. *Arch. Oral Biol. 50*, 599–609.

(43) Kawasaki, K., and Weiss, K. M. (2003) Mineralized tissue and vertebrate evolution: The secretory calcium-binding phosphoprotein gene cluster. *Proc. Natl. Acad. Sci. U.S.A. 100*, 4060–4065.

(44) Kawasaki, K., and Weiss, K. M. (2006) Evolutionary genetics of vertebrate tissue mineralization: The origin and evolution of the secretory calcium-binding phosphoprotein family. *J. Exp. Zool., Part B 306*, 295–316.

(45) Dunker, A. K., Brown, C. J., Lawson, J. D., Iakoucheva, L. M., and Obradović, Z. (2002) Intrinsic disorder and protein function. *Biochemistry 41*, 6573–6582.

(46) Schröder, H. C., Boreiko, A., Korzhev, M., Tahir, M. N., Tremel, W., Eckert, C., Ushijima, H., Müller, I. M., and Müller, W. E. G. (2006) Co-expression and functional interaction of silicatein with galectin: Matrix-guided formation of siliceous spicules in the marine demosponge *Suberites domuncula*. *J. Biol. Chem. 281*, 12001–12009.

(47) Lemmon, M. A. (2004) Pleckstrin homology domains: Not just for phosphoinositides. *Biochem. Soc. Trans. 32*, 707–711.

(48) Lemmon, M. A., and Ferguson, K. M. (2000) Signal-dependent membrane targeting by pleckstrin homology (PH) domains. *Biochem. J. 350*, 1–18.

(49) Blomberg, N., Baraldi, E., Sattler, M., Saraste, M., and Nilges, M. (2000) Structure of a PH domain from the *C. elegans* muscle protein UNC-89 suggests a novel function. *Structure 8*, 1079–1087.

(50) Fröhlich, H., and Bartel, D. (1997) Silica uptake of the *Halichondria panicea* in Kiel Bight. *Mar. Biol. 128*, 115–125.

(51) Schröder, H. C., Perović-Ottstadt, S., Rothenberger, M., Wiens, M., Schwertner, H., Batel, R., Korzhev, M., Müller, I. M., and Müller, W. E. G. (2004) Silica transport in the demosponge *Suberites domuncula*: Fluorescence emission analysis using the PDMPO probe and cloning of a potential transporter. *Biochem. J. 381*, 665–673.

(52) Vinogradov, A. P. (1953) *The Elementary Chemical Composition of Marine Organisms* (translated by J. Efron and J. K. Setlow), Sears Foundation for Marine Research, New Haven, CT.

(53) Gross, J., Sokal, Z., and Rougvie, M. (1956) Structural and chemical studies on the connective tissue of marine sponges. *J. Histochem. Cytochem. 4*, 227–236.